

Performance of circular patch microstrip antenna for adaptive modulation and coding applications

Hiba A. Alsawaf¹, Bushra Muhammed Ahmad²

¹Department of Electronic Engineering, Electronics Engineering College, Ninevah University, Mosul, Iraq

²Department of Electrical Engineering, Engineering College, University of Mosul, Mosul, Iraq

Article Info

Article history:

Received Nov 22, 2021

Revised Mar 10, 2022

Accepted Apr 8, 2022

Keywords:

Circular antenna

Gain

HFSS

Radiation pattern

Return loss

ABSTRACT

The thickness of the substrate is one factor influencing antenna performance. In this paper, the circular patch antenna was designed using Rogers RT5880 with dielectric constant of 2.20, loss kept 0.0009 and FR-epoxy with dielectric constant of 4.4, loss kept 0.02. The thickness of the substrate was varied to see how it affected antenna performance, such as return loss. The thickness of the checked substrate is 1.58 mm, which is the standard thickness for Rogers RT5880 as well as 2.08 mm, 2.58 mm and 2.85 mm. The simulation work is carried out by ANSYS HFSS software. In this paper, the thicknesses of different substrates are checked while other parameters stay constant and the circular patch radius of the antennas is optimized to achieve a resonant frequency of 3.5 GHz based on the thickness of the above-mentioned substrates used. Return loss, VSWR, gain and half power beam width were found, and the results showed that with the increase in the thickness of the substrate, the gain increases and the value of half power beam width (HPBW) and better results were obtained in the case of RTduroid 5880 and for thicknesses $h=2.85$ mm.

This is an open access article under the [CC BY-SA](https://creativecommons.org/licenses/by-sa/4.0/) license.



Corresponding Author:

Hiba A. Alsawaf

Department of Electronic Engineering, Electronics Engineering College, Ninevah University

85H2+VCM, Mosul, Iraq

Email: hiba.hmduon@uoninevah.edu.iq

1. INTRODUCTION

Antennas with a small footprint and the ability to operate across multiple frequency bands have generated a lot of interest in recent years, especially for novel wireless communication systems such as radio frequency identification [1], microwave-based global interoperability and wireless local area networks (WLAN). (WiMAX) [2]–[7], among which are applications modification and adaptive coding. Multiband antennas should operate in the appropriate frequency ranges for these applications: 2.45 GHz (2.40–2.50 GHz), 3.5 GHz (3.40–3.70 GHz), and 5.8 GHz (5.725–5.875 Hz) [8]. The 3.5 GHz frequency was selected for this study. Microstrip antennas offer a wide range of uses, including medical, military, mobile, and satellite communication [9]–[13]. As wireless applications need greater capacity, wideband antennas operating at higher frequencies are unavoidable [14]–[21]. The efficiency of microstrip antennas is low, and their bandwidth is small, and substrate parameters like dielectric constant, homogeneity, and tangent loss impact their performance [22]–[25]. The need for wideband antennas operating at higher frequencies is growing rapidly as more wireless applications require greater bandwidth [26]. Broadside radiators make up the vast bulk of microstrip antennas [27]. Patches of printed antennas' radiating elements come in a diverse range of shapes, including rectangle, square, elliptical, and circular shape [28]–[31]. A suitable model selection can also be used to select an end-fire radiator [32], [33]. At microwave frequencies ($f > 1$ GHz), a microstrip patch

antenna is one of the most useful antennas. It comprises a metal "patch" above the insulating substrate and a ground plane beneath the insulating layer. The feed position must be altered to adjust the input impedance as previously [34]–[36]. Thicker substrates with lower dielectric constants are more efficient, have a bigger bandwidth, enhance the patch's fringing field and hence radiating power, but add weight and surface wave losses [37]. A patch antenna can be fed in various ways, including probe feed, microstrip line feed, aperture coupled feed, and proximity coupling feed [38]. Saidulu *et al.* [39] focused on the circular patch-fed axial probe of microstrip antenna properties with and without a dielectric substrate. As the return loss and VSWR increase, the bandwidth and gain decrease with the dielectric constant of the super-substrates. According to Hamzah *et al.* [40] the circular patch antenna is built using a Rogers RT5880 with a tangent loss of 0.0009 and 2.2 is the dielectric constant. The purpose of this study was to see how the thickness of the substrate affected the performance of the antenna, i.e. thickness of that substrate has been modified, resulting in a change in return loss. CST microwave studio conducted the simulations. Research by Sharma *et al.* [41] used the ultra-high frequency (UHF) band from 470MHz to 806MHz and developed the circular microstrip patch antenna used for this band. The pin from the center is used to shorten the main patch. Sateaa *et al.* [42] presented (3) rectangular microstrip patch array antennas ((1*1), (1*2), and (1*4)) with easy and small construction. The suggested antenna was designed utilizing (CST) and printed on a Rogers RT5880 (lossy) substrate with a dielectric constant of 2.2, a loss tangent of 0.0009, and a thickness of 0.1 mm. The patch size is (1.570 mm*2 mm) for three designs of microstrip patch array antenna, and it operates in dual-band. Thakur and Singh [43] proposed a novel photonic band gap substrate-based microstrip patch antenna for cancer detection. With a gain of 3.430 dBi and a reflection coefficient of -68.530 dB, the antenna resonates at 0.198 THz. According to Jairath *et al.* [44] the antenna designed in this study exhibits an impedance bandwidth across the ultrafast bandwidth (UWB) frequency range of 3.10 to 14 GHz with a constant voltage wave ratio of less than 2, excluding the band stops at 3.29 to 3.70GHz (WiMAX band), 3.70 to 4.10 GHz (C band), 5.10 to 5.90GHz (WLAN band), and 7.060 to 7.76 GHz (downlink X band satellite communication). The suggested antenna, which is built on a low-cost FR-4 substrate, has a small footprint of (24*20*1.6) mm³. Jairath and Singh [45] presented a novel WLAN and X-band frequency rejected antenna with an elliptical slot in the radiating patch and a metamaterial inspired strict source and record route SSR strip. The antenna reported in this study has a low voltage standing wave ratio at the rejected frequency ranges (5.150–5.825GHz), (7.360–8.06GHz), and (9.54–10.38GHz).

The used high frequency simulation software high-frequency structure simulator (HFSS) program to develop the design, which was set to 3.5 GHz. In the circular antenna, two substrates were employed, with thicknesses of 1.58 mm, 2.08 mm, 2.58 mm and 2.85 mm for each substrate. This paper is organized as: section 2 deals with the proposed circular antenna. The third section shows the method for calculating the parameters of the designed circular antenna. The results are presented and discussed for the designed antenna, for two types of RT/duroid5880 and Fr epoxy substrates with thicknesses of 1.58 mm, 2.05 mm, 2.58 mm and 2.85 mm in the fourth section. The fifth section contains the conclusions.

2. RESEARCH METHOD

The suggested antenna dimensions are computed using the operating frequency, f_r , of 3.5 GHz, the height of the substrate of 1.58 mm, 2.05 mm, 2.58 mm and 2.85 mm, the dielectric permittivity of the Fr-epoxy and RT5880 substrates, of 2.20 for RT5880 and 4.4 for Fr-epoxy, as shown in Table 1.

Table 1. Antenna design specifications for microstrip circular patch

Parameters for antenna design	Specifications							
Frequency of operation	3.5 GHz	3.5 GHz	3.5 GHz	3.5 GHz	3.5 GHz	3.5 GHz	3.5 GHz	3.5 GHz
Substrate	Fr-epoxy ($\epsilon_r=4.4$)	Fr-epoxy ($\epsilon_r=4.4$)	Fr-epoxy ($\epsilon_r=4.4$)	Fr-epoxy ($\epsilon_r=4.4$)	RT-duroid 5880. ($\epsilon_r=2.20$)	RT-duroid 5880. ($\epsilon_r=2.20$)	RT- duroid 5880. ($\epsilon_r=2.20$)	RT-duroid 5880. ($\epsilon_r=2.20$)
Thickness of substrate(h)	1.58 mm	2.05 mm	2.58 mm	2.85 mm	1.58 mm	2.05 mm	2.58 mm	2.85 mm
Tangent factor	0.02	0.02	0.02	0.02	0.0009	0.0009	0.0009	0.0009

Microstrip circular patch antenna using fr epoxy and RT-duroid 5880 is designed using HFSS software and analysis has been carried out to determine the design parameter to achieve the adaptive modulation and coding applications requirements. Figure 1 shows the proposed microstrip circular patch antenna designed using HFSS. Circular geometries have benefits over conventional geometries in some applications, such as arrays, because the feed may be linked at any point along the circumference. The basic antenna design equations are given step by step as:

a. The radius of the circular patch antenna (R)

$$R = \frac{F}{\sqrt{1 + \frac{2h}{\pi \cdot \epsilon_r \cdot F \left[\ln\left(\frac{F\pi}{2h}\right) + 1.7726 \right]}}} \quad (1)$$

$$F = \frac{8.791 \cdot 10^9}{f_{res} \sqrt{\epsilon_r}} \quad (2)$$

Where h is substrate height and ϵ_r is substrate dielectric constant

b. Microstrip line width

$$\frac{w}{h} = \begin{cases} \frac{8e^K}{e^{2K}-2} \text{ for } \frac{w}{h} < 2 \\ \frac{2}{\pi} \left[P - 1 - (2P - 1) + \frac{\epsilon_r - 1}{2\epsilon_r} \left\{ \ln(P - 1) + 0.39 - \frac{0.61}{\epsilon_r} \right\} \right] \text{ for } \frac{w}{h} > 2 \end{cases} \quad (3)$$

$$K = \frac{Z_0}{60} \sqrt{\frac{\epsilon_r + 1}{2}} + \frac{\epsilon_r - 1}{\epsilon_r + 1} \left(0.23 + \frac{0.11}{\epsilon_r} \right) \text{ and } P = \frac{377\pi}{2Z_0\sqrt{\epsilon_r}} \quad (4)$$

where Z_0 is line impedance

Using the in (3) and (4), the width of the 50 line (W_1) and the width of the transformer line (W_2) may be determined.

c. Quarter wave transformer length

$$L = \frac{\lambda_d}{4} = \frac{\lambda_0}{4\sqrt{\epsilon_{ref}}} \quad (5)$$

$$\frac{\epsilon_r + 1}{2} + \frac{\epsilon_r - 1}{2} \left(1 + \frac{12h}{w} \right)^{-0.5} \quad (6)$$

Where λ_0 is wavelength of free space and λ_d is dielectric substrate of wavelength

d. Radiation losses conductance (G_R)

$$G_R = \frac{2.39}{4 \cdot h \cdot f_0 \cdot \mu_0 \cdot Q_R} \quad (7)$$

$$Q_R = \frac{4 \cdot R (\alpha_{11}^2 - 1) \cdot \epsilon^{\frac{3}{2}}}{h \cdot \alpha_{11}^3 \cdot F\left(\frac{\alpha_{11}}{\sqrt{\epsilon_r}}\right)} \quad (8)$$

Where ϵ_r is dielectric constant, $\alpha_{11}=1.84118$, and R is radius of circular patch

e. Dielectric losses conductance (G_D)

$$G_D = \frac{2.39 \cdot \tan \delta}{4 \mu_0 \cdot h \cdot f_0} \quad (9)$$

f. Conduction (ohmic) losses conductance (G_C)

$$G_C = \frac{2.39 \cdot \pi \cdot (\pi \cdot \mu_0 \cdot f_0)}{4 \cdot h^2 \cdot \sqrt{\sigma}} \quad (10)$$

Where σ is conductance of copper material used in design ($5.8 \cdot 10^7$) and $\mu_0 = 1.256 \cdot 10^{-6}$

$$G_T = G_R + G_D + G_C \quad (11)$$

g. The impedance of quarter wave transformer (Z_{tr})

$$Z_{tr} = \sqrt{Z_T \cdot Z_0} \quad (12)$$

Where Z_0 is characteristic impedance of feed line and Z_{tr} is impedance of $\lambda/4$ transformer

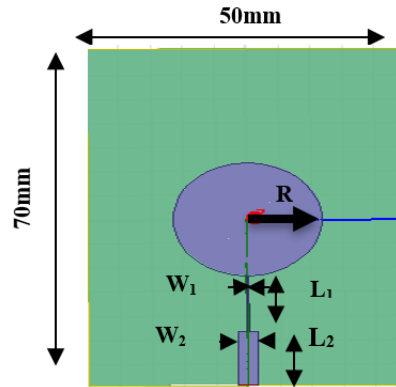


Figure 1. Circular microstrip antenna edge feeding

To match a 50 feed transmission line with the circular microstrip patch, a quarter-wave transformer is used. A quarter-wave transformer is a simple impedance transformer used in impedance matching to decrease the energy reflected when a transmission line is connected to a load. The needed calculations for the circular antenna sections are shown in Table 2.

Table 2. Calculations of circular microstrip antenna with edge feeding for eight substrates

Parameter	Fr epoxy ($\epsilon_r=4.4$, $h=1.58$ mm)	Fr epoxy ($\epsilon_r=4.4$, $h=2.08$ mm)	Fr epoxy ($\epsilon_r=4.4$, $h=2.58$ mm)	Fr epoxy ($\epsilon_r=4.4$, $h=2.85$ mm)	RT- duroid 5880. ($h=1.58$ mm, $\epsilon_r=2.20$)	RT- duroid 5880. ($h=2.08$ mm, $\epsilon_r=2.20$)	RT- duroid 5880. ($h=2.58$ mm, $\epsilon_r=2.20$)	RT- duroid 5880. ($\epsilon_r=2.20$, $h=2.85$ mm)
Patch radius (mm)	11.7	11.55	11.38	11.25	16.21	16.1	16.05	15.7
Length of the $\lambda/4$ transformer (L_1) mm	11.74	12.065	12.109	12.717	16.41	15.52	15.523	16.3012
Width of the $\lambda/4$ transformer (W_1) mm	0.253	0.31	0.4236	0.452	0.611	0.877	1.255	1.104
50 Ω line length (L_2) mm	11.183	11.183	11.183	11.1832	14.919	14.919	14.919	14.919
50 Ω line width (W_2) mm	3.036	3.976	4.932	5.4532	4.883	6.4088	7.949	8.627
GR (Siemens)	8.853×10^{-4}	8.446×10^{-4}	8.446×10^{-4}	8.446×10^{-4}	2.478×10^{-3}	3.377×10^{-3}	3.376×10^{-3}	3.375×10^{-3}
GD (Siemens)	1.7118×10^{-3}	1.3069×10^{-3}	1.053×10^{-3}	9.708×10^{-4}	7.7031×10^{-5}	5.881×10^{-5}	4.7413×10^{-5}	4.368×10^{-5}
GC (Siemens)	6.2413×10^{-5}	3.51×10^{-5}	2.281×10^{-5}	1.937×10^{-5}	6.022×10^{-5}	3.51×10^{-5}	2.281×10^{-5}	1.937×10^{-5}
GT (Siemens)	26.5957×10^{-4}	21.866×10^{-4}	19.2041×10^{-4}	18.3477×10^{-4}	2.616×10^{-3}	3.47091×10^{-3}	3.446×10^{-3}	3.438×10^{-3}
ZT (Ω)	376	457.331	520.722	545.027	382.26	288.108	290.17	290.862
Ztr (Ω)	137.113	151.216	161.357	165.079	138.242	120.022	120.45	120.594

3. RESULTS AND DISCUSSION USING HIGH-FREQUENCY STRUCTURE SIMULATOR

3.1. Result of circular microstrip antenna using Fr epoxy ($h=1.58$ mm, $h=2.08$, $h=2.58$ mm and $h=2.85$ mm with $\epsilon_r=4.4$)

The Figure 2 shows return loss plot for circular microstrip antenna with four thicknesses ($h=1.58$ mm, $h=2.08$, $h=2.58$ mm and $h=2.85$ mm, $\epsilon_r=4.4$), Where the better return loss value Fr epoxy ($h=2.85$ mm) is (-22.4776 dB). The VSWR of circular microstrip antenna with four thicknesses are seen in Figure 3. As can be seen in Figure 4 (in appendix) the gain value of circular antenna with four thicknesses, where Figure 4(a) for $h=1.58$ mm, Figure 4(b) for $h=2.05$ mm, Figure 4(c) for $h=2.58$ mm and Figure 4(d) for $h=2.85$ mm). Figure 5 (in appendix) depicts the circular antenna's radiation pattern, which was used to determine the half-

power beam width, where Figure 5(a) for $h=1.58$ mm, Figure 5(b) for $h=2.08$ mm, Figure 5(c) for $h=2.58$ mm, and Figure 5(d) for $h=2.85$ mm.

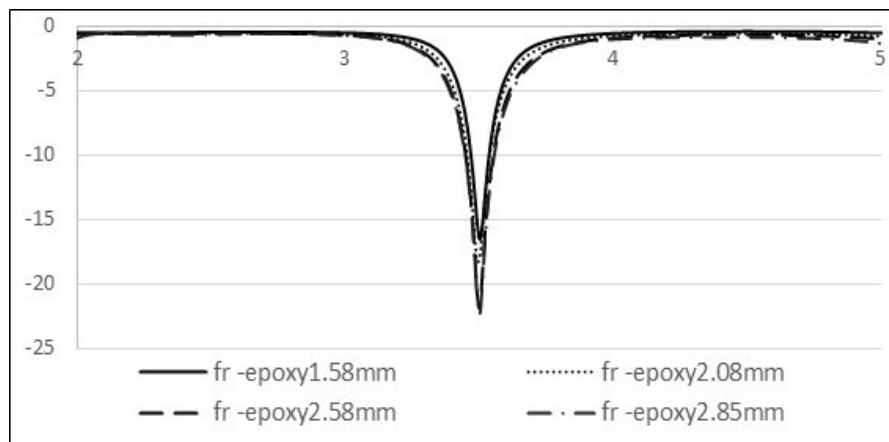


Figure 2. Circular microstrip antenna return loss for Fr-epoxy with $\epsilon_r=4.4$

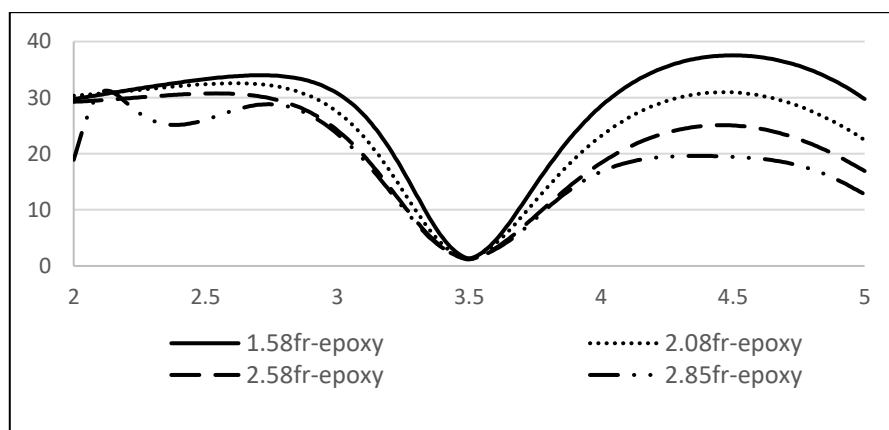


Figure 3. VSWR of circular microstrip antenna for Fr-epoxy with $\epsilon_r=4.4$

3.2. Result of circular microstrip antenna using Rogers RT/Duroid5880 ($h=1.58$ mm, $h=2.08$ mm, $h=2.58$ mm and $h=2.85$ mm with $\epsilon_r=2.20$)

Figure 6 illustrates a return loss plot for a circular microstrip antenna with four thicknesses ($h=1.58$ mm, $h=2.08$, $h=2.58$ mm and $h=2.85$ mm, with $\epsilon_r=2.20$). Figure 7 shows the VSWR of a circular microstrip antenna with four thicknesses ($h=1.58$ mm, $h=2.08$, $h=2.58$ mm and $h=2.85$ mm, with $\epsilon_r=2.20$). Figure 8 (in appendix) shows a circular microstrip antenna's gain when fed from the edge for RT Duroid5880 with four thicknesses, where Figure 8(a) for $h=1.58$ mm, Figure 8(b) for $h=2.05$ mm, Figure 8(c) for $h=2.58$ mm and Figure 8(d) for $h=2.85$ mm). Figure 9 (in appendix) demonstrates a circular microstrip antenna's radiation pattern for RT Duroid5880, Figure 9(a) shows (RT Duroid5880 ($h=1.58$ mm, $\epsilon_r=2.20$)), Figure 9(b) shows (RT Duroid5880 ($h=2.08$ mm, $\epsilon_r=2.20$)), Figure 9(c) shows (RT Duroid5880 ($h=2.58$ mm, $\epsilon_r=2.20$)), and Figure 9(d) shows (RT Duroid5880 ($h=2.85$ mm, $\epsilon_r=2.20$)).

Table 3 summarizes the modeling findings for these four substrates at 3.5GHz (in appendix). The circular antenna with substrate Rogers RT Duroid5880 and the 4 suggested thicknesses has superior performance than the circular antenna with Fr epoxy substrate, as shown in Table 3. It's worth noting that as the substrates' thickness gets thicker, the gain and HPBW improve. The greatest gain is 8.0998 dB for Rogers RT Duroid5880 ($\epsilon_r=2.2$, $h=2.85$ mm). When the thickness is increased, the return losses and VSWR of the Fr epoxy substrate are better than that of Rogers RT Duroid5880 substrate. Figures 10 to 17 show the priority of RT Duroid5880 over Fr-Epoxy in terms of VSWR, Returnloss for all cases used in the design.

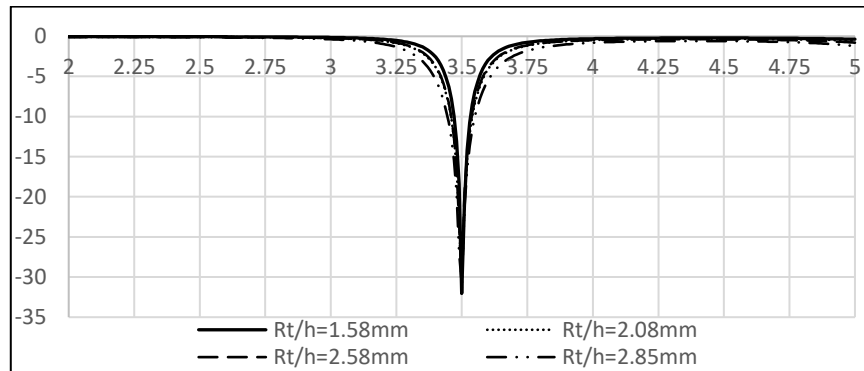


Figure 6. Circular microstrip antenna return loss for RT/Duroid5880 with $\epsilon_r=2.20$

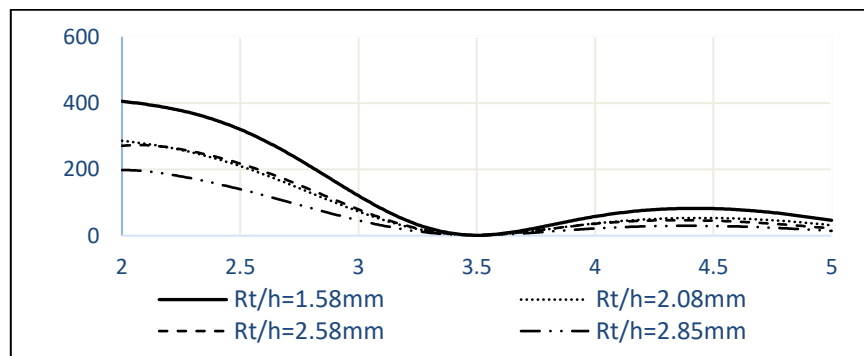


Figure 7. VSWR of circular microstrip antenna for RT duroid5880 with $\epsilon_r=2.20$

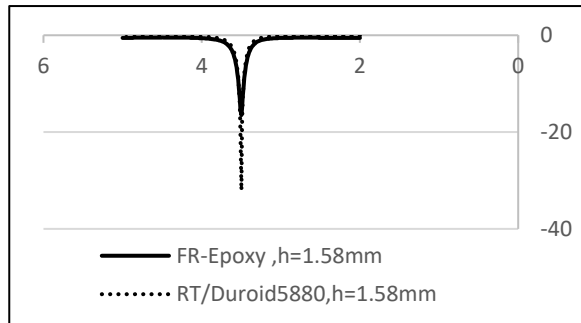


Figure 10. Comparison circular microstrip antenna return loss between Fr-epoxy and RT/duroid5880, ($h=1.58$ mm)

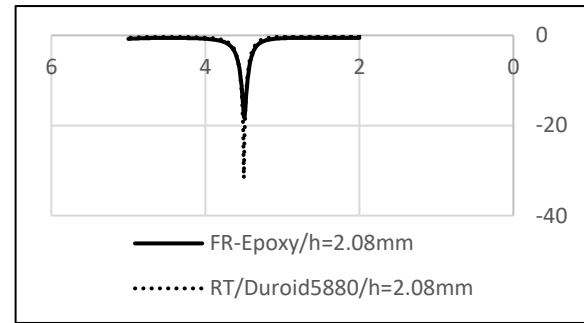


Figure 11. Comparison circular microstrip antenna return loss between Fr-epoxy and RT/duroid5880, ($h=2.08$ mm)

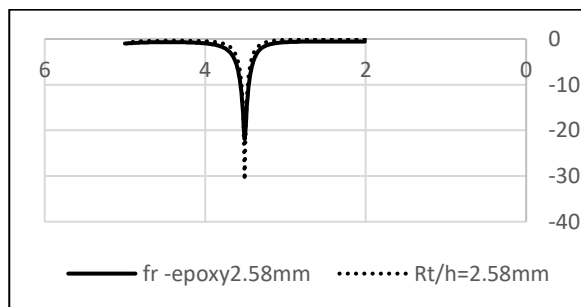


Figure 12. Comparison circular microstrip antenna return loss between Fr-epoxy and RT/duroid5880, ($h=2.58$ mm)

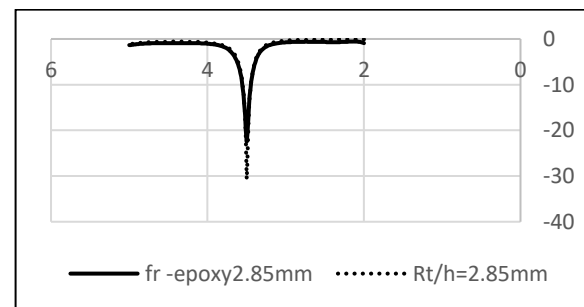


Figure 13. Comparison circular microstrip antenna return loss between Fr-epoxy and RT/duroid5880, ($h=2.85$ mm)

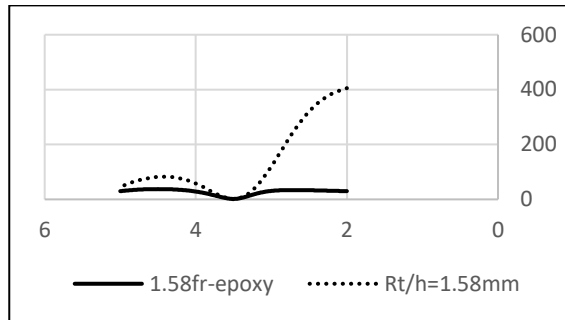


Figure 14. Comparison of VSWR for circular microstrip antenna between Fr-epoxy and RT/duroid5880, ($h=1.58$ mm)

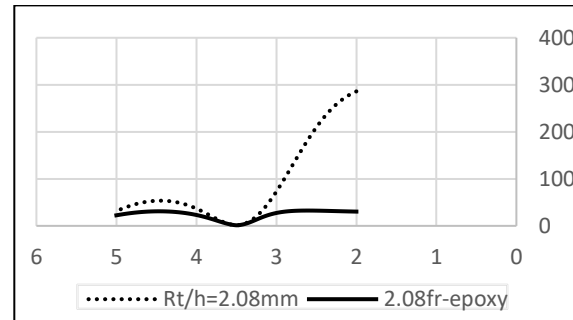


Figure 15. Comparison of VSWR for circular microstrip antenna between Fr-epoxy and RT/duroid5880, ($h=2.08$ mm)

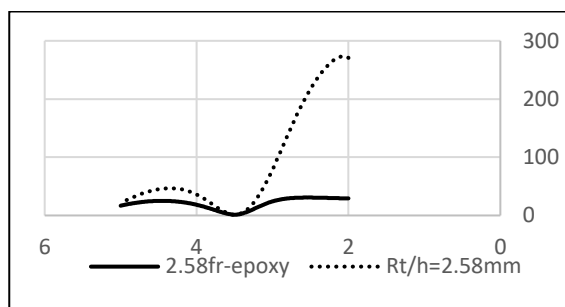


Figure 16. Comparison of VSWR for circular microstrip antenna between Fr-epoxy and RT/duroid5880, ($h=2.58$ mm)

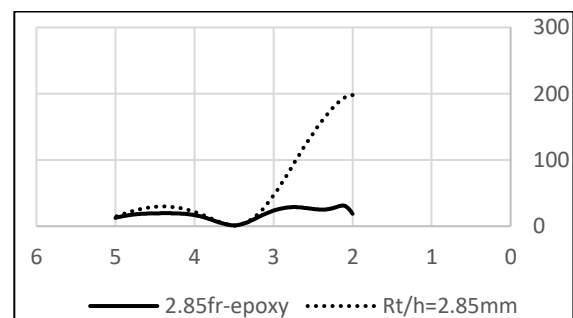


Figure 17. Comparison of VSWR for circular microstrip antenna between Fr-epoxy and RT/duroid5880, ($h=2.85$ mm)

4. CONCLUSION

The HFSS 15.0 simulation program is used to create a circular antenna that resonates at 3.5GHz. Eight circular microstrip antennas were designed with Fr epoxy ($\epsilon_r=4.4$, $h=1.58$ mm), Fr epoxy ($\epsilon_r=4.4$, $h=2.08$ mm), Fr epoxy ($\epsilon_r=4.4$, $h=2.58$ mm), Fr epoxy ($\epsilon_r=4.4$, $h=2.85$ mm), Rogers RT/duroid5880 ($\epsilon_r=2.20$, $h=1.58$ mm), Rogers RT/duroid5880 ($\epsilon_r=2.20$, $h=2.08$ mm), Rogers RT/duroid5880 ($\epsilon_r=2.20$, $h=2.58$ mm) and Rogers RT/duroid5880 antennas ($\epsilon_r=2.20$, $h=2.85$ mm). The results indicated the superior performance of the circular antenna with Rogers RT/duroid5880 ($\epsilon_r=2.20$, $h=2.85$ mm) in terms of gain and HPBW, the gain value equals 8.0998db and HPBW equals 63.2888dB.

ACKNOWLEDGEMENTS

We would like to express gratitude to the College of Electronics Engineering/Ninevah University and College of Engineering/University of Mosul.

APPENDIX

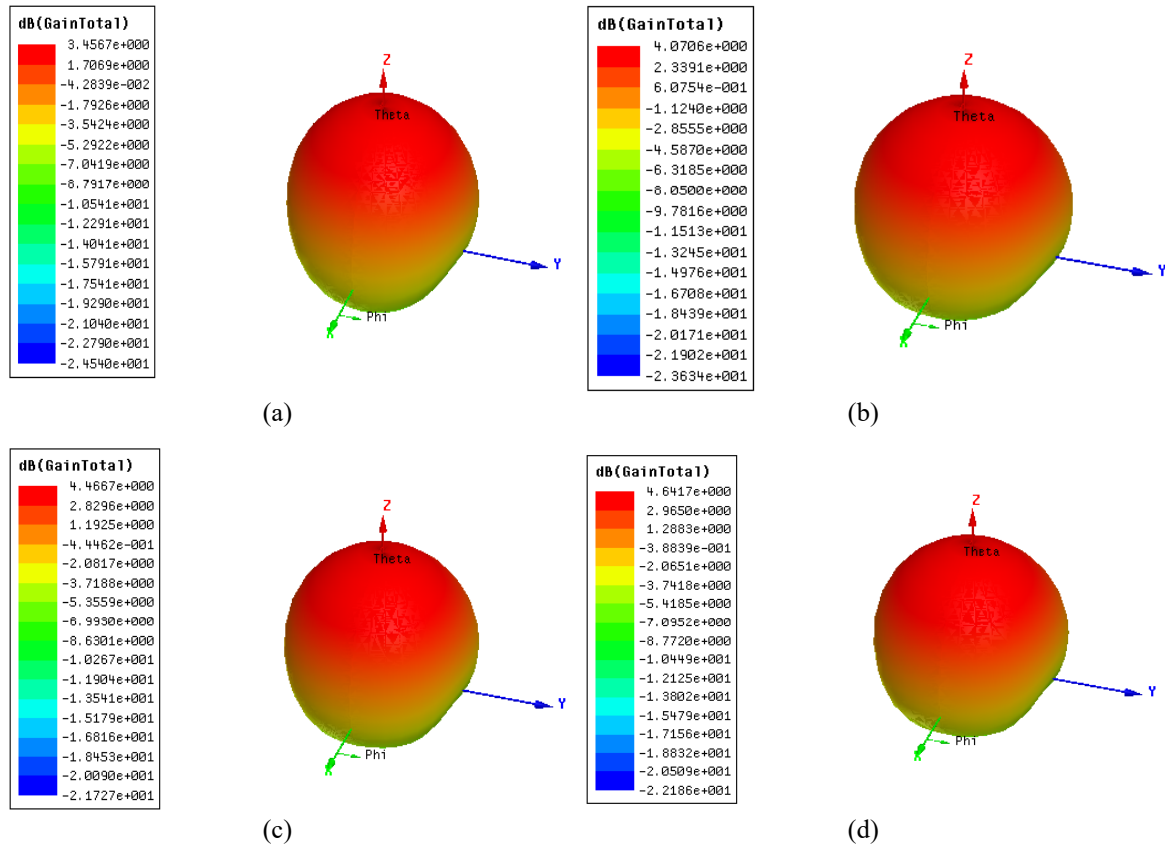


Figure 4. Gain of circular microstrip antenna (a) (Fr epoxy (h=1.58 mm, Cr=4.4)), (b) (Fr epoxy (h=2.08 mm, Cr=4.4)), (c) (Fr epoxy (h=2.58 mm, Cr=4.4)) and (d) (Fr epoxy (h=2.85 mm, Cr=4.4))

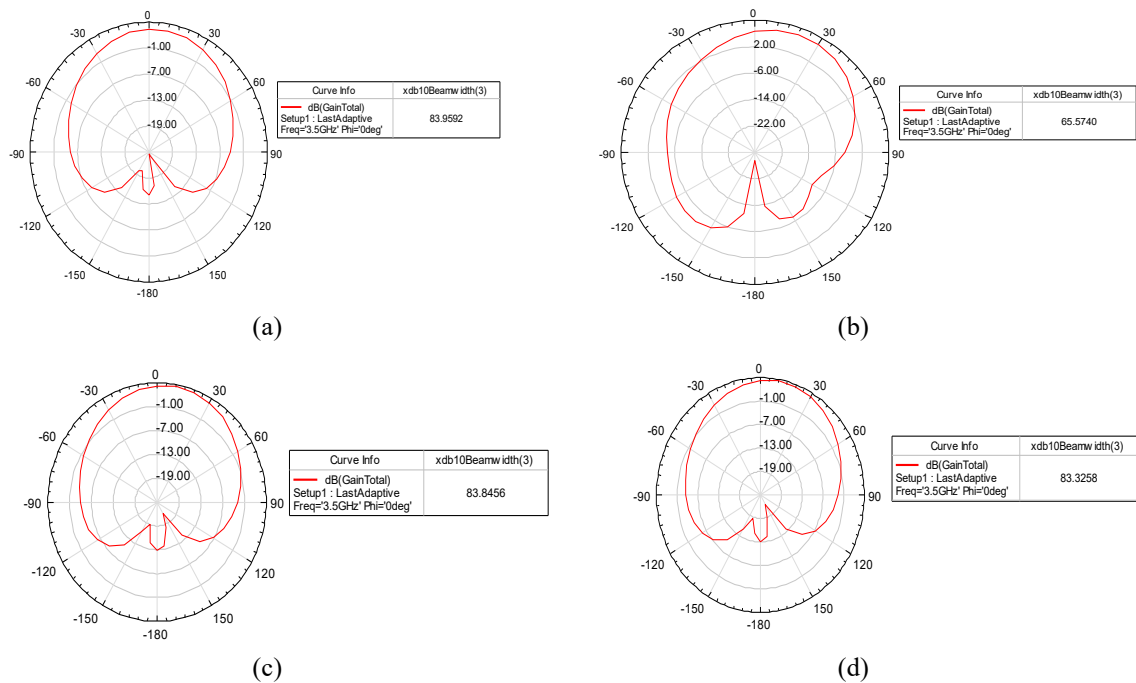


Figure 5. Radiation pattern of circular microstrip antenna, (a) (Fr epoxy (h=1.58 mm, Cr=4.4)), (b) (Fr epoxy (h=2.08 mm, Cr=4.4)), (c) (Fr epoxy (h=2.58 mm, Cr=4.4)) and (d) (Fr epoxy (h=2.85 mm, Cr=4.4))

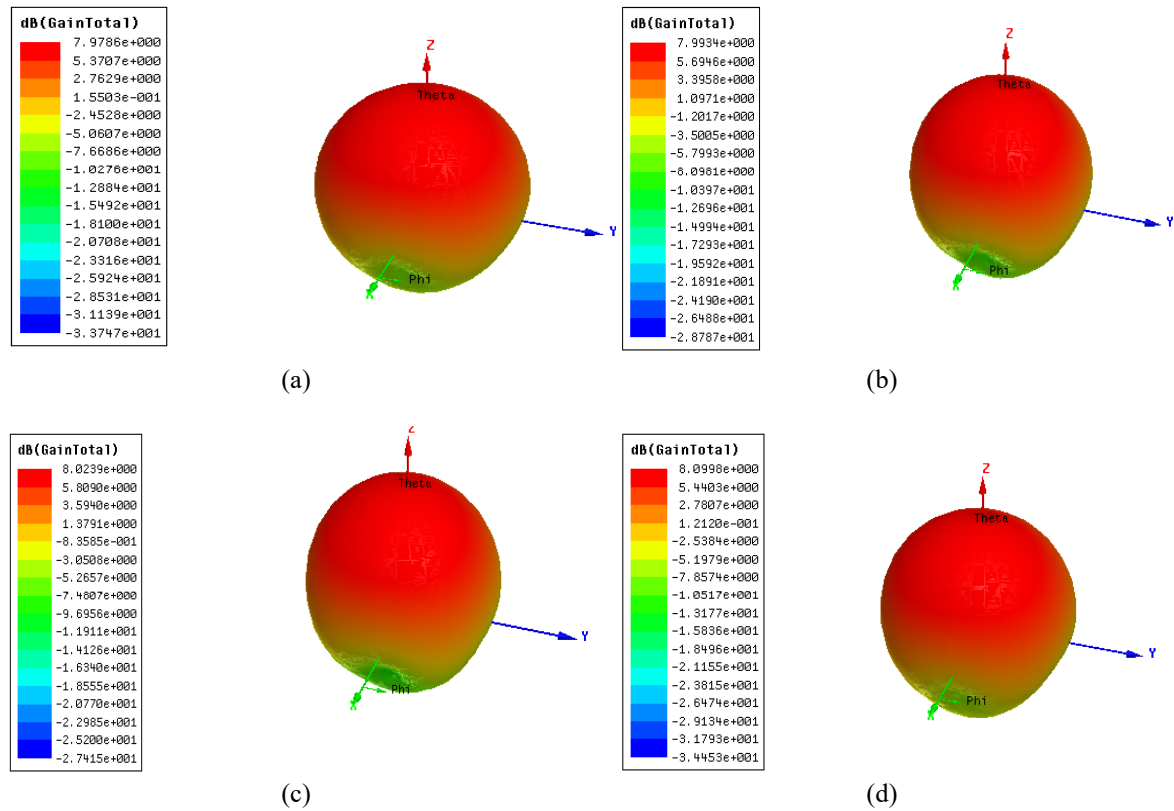


Figure 8. Gain of circular microstrip antenna (a) RT duroid5880 ($h=1.58$ mm, $\epsilon_r=2.20$), (b) RT duroid5880 ($h=2.08$ mm, $\epsilon_r=2.20$), (c) RT duroid5880 ($h=2.58$ mm, $\epsilon_r=2.20$), and (d) RT duroid5880 ($h=2.85$ mm, $\epsilon_r=2.20$)

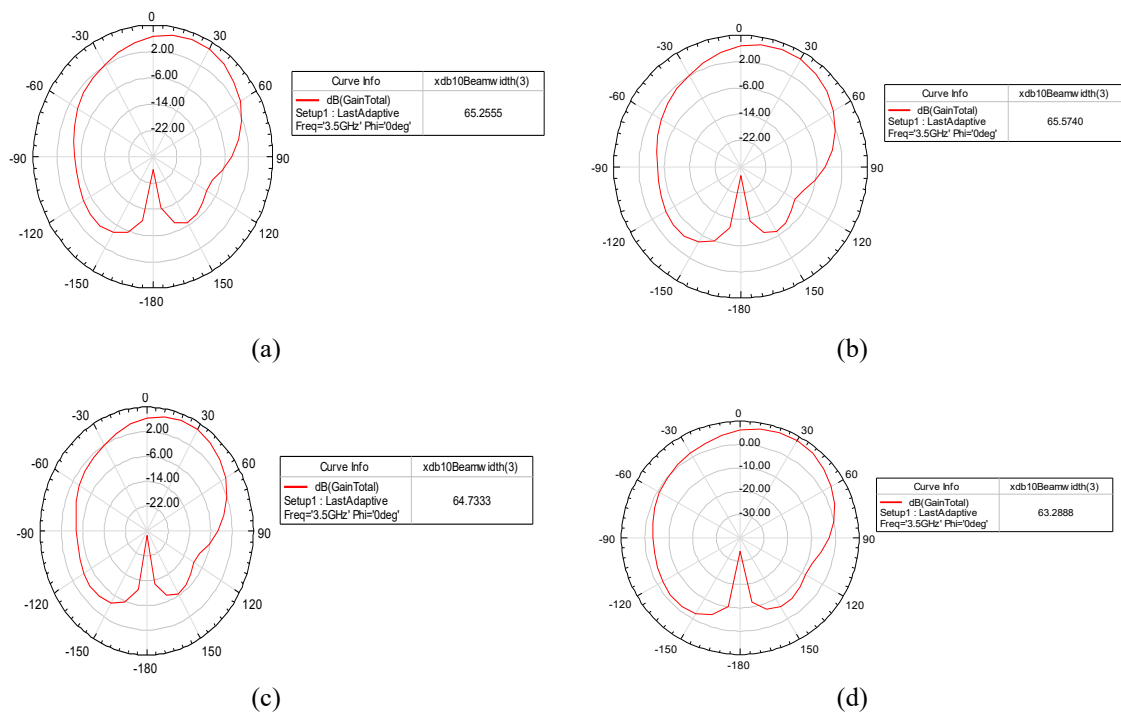


Figure 9. Radiation pattern of circular microstrip antenna, (a) (RT duroid5880 ($h=1.58$ mm, $\epsilon_r=2.20$)), (b) (RT duroid5880 ($h=2.08$ mm, $\epsilon_r=2.20$)), (c) (RT Duroid5880 ($h=2.58$ mm, $\epsilon_r=2.20$)) and (d) (RT duroid5880 ($h=2.85$ mm, $\epsilon_r=2.20$))

Table 3. Results circular microstrip antenna for four substrates

Parameter	Fr epoxy ($\epsilon_r=4.4$, $h=1.58$ mm)	Fr epoxy ($\epsilon_r=4.4$, $h=2.08$ mm)	Fr epoxy ($\epsilon_r=4.4$, $h=2.58$ mm)	Fr epoxy ($\epsilon_r=4.4$, $h=2.85$ mm)	RT- duroid 5880. ($h=1.58$ mm, $\epsilon_r=2.20$)	RT- duroid 5880. ($h=2.08$ mm, $\epsilon_r=2.20$)	RT- duroid 5880. ($h=2.58$ mm , $\epsilon_r=2.20$)	RT- duroid 5880. ($\epsilon_r=2.2$, $h=2.85$ mm)
VSWR	1.3518	1.2848	1.1734	1.1626	1.0513	1.0535	1.0585	1.0599
Return loss (dB)	-16.5015	-18.0866	-21.2606	-22.4776	-32.0420	-31.6891	-30.9252	-30.7227
Gain (dB)	3.4567	4.0706	4.4667	4.6417	7.9786	7.9934	8.0239	8.0998
Half power beam width(dB)	83.9592	83.9413	83.8456	83.5451	65.2555	65.5740	64.7333	63.2888





REFERENCES

- [1] A. Ennajih, B. Nasiri, J. Zbitou, A. Errkik, and M. Latrach, "A wearable UHF RFID tag antenna-based metamaterial for biomedical applications," *Bulletin of Electrical Engineering and Informatics*, vol. 9, no. 2, pp. 676-684, 2020, doi: 10.11591/eei.v9i2.1661.
- [2] Z. Mousavirazi, V. Rafiei, and T. A. Denidni, "Beam-Switching antenna array with dual-circular-polarized operation for WiMAX applications," *AEU-International Journal of Electronics and Communications*, vol. 137, p. 153796, 2021, doi: 10.1016/j.aeeu.2021.153796.
- [3] F. Fertas, M. Challal, and K. Fertas, "A compact slot-antenna with tunable-frequency for WLAN, WiMAX, LTE, and X-band applications," *Progress In Electromagnetics Research C*, vol. 102, pp. 203-212, 2020, doi:10.2528/PIERC20020304.
- [4] P. Nayak, "Triple Band Antenna Design for Bluetooth, WLAN and WiMAX Applications," *Indian Institute of Technology Patna*, 2021.
- [5] J. kaithan Shadkh, R. M. Shaaban, and R. e. Malallah, "Design and Analysis of Double-Band Printed Corrugated Circular Patch Antenna for Wireless Communication Applications," *Basrah Journal of Science*, vol. 39, no. 3, pp. 432-445, 2021.
- [6] M. A. Baba *et al.*, "A compact triband microstrip antenna utilizing hexagonal CSRR for wireless communication systems," *Bulletin of Electrical Engineering and Informatics*, vol. 9, no. 5, pp. 1916-1923, 2020, doi: 10.11591/eei.v9i5.2191.
- [7] G. Sowmya, A. Kamath, A. Keshava, O. P. Kumar, S. Vincent, and T. Ali, "A circular monopole patch antenna loaded with inverted L-shaped stub for GPS application," *Bulletin of Electrical Engineering and Informatics*, vol. 9, no. 5, pp. 1950-1957, 2020, doi: 10.11591/eei.v9i5.2357.
- [8] I. Fatima, A. Ahmad, S. Ali, M. Ali, and M. I. Baig, "Triple-Band Circular Polarized Antenna for WLAN/WiFi/Bluetooth/WiMAX Applications," *Progress in Electromagnetics Research C*, vol. 109, pp. 65-75, 2021, doi:10.2528/PIERC20121207.
- [9] N. Zaidi, M. Ali, N. Abd Rahman, M. Yahya, and M. A. Nordin, "Analysis on different shape of textile antenna under bending condition for GPS application," *Bulletin of Electrical Engineering and Informatics*, vol. 9, no. 5, pp. 1964-1970, 2020, doi: 10.11591/eei.v9i5.2185.
- [10] V. Prakasam, K. A. LaxmiKanth, and P. Srinivasu, "Design and simulation of circular microstrip patch antenna with line feed wireless communication application," *4th International Conference on Intelligent Computing and Control Systems (ICICCS)*, 2020, pp. 279-284, doi: 10.1109/ICICCS48265.2020.9121162.
- [11] R. Shirbhate, D. D. Dhumal, and A. Keskar, "Dual-Band Microstrip Patch Antenna for Wireless Communication," *Proceedings of First International Conference on Computational Electronics for Wireless Communications*, 2022, vol. 329, pp. 47-57.
- [12] F. Al-Janabi, M. J. Singh, and A. P. S. Phawaha, "Development of Microstrip Antenna for Satellite Application at Ku/Ka Band," *Journal of Communications*, vol. 16, no. 4, pp. 118-125, 2021, doi:10.12720/jcm.16.4.118-125.
- [13] Z. Rahman Md and M. Mohammed, "Design and Simulation of High Performance Rectangular Microstrip Patch Antenna Using CST Microwave Studio," *GSI*, 2020.
- [14] A. Wa'il, R. M. Shaaban, and A. Tahir, "Design, simulation and measurement of triple band annular ring microstrip antenna based on shape of crescent moon," *AEU-International Journal of Electronics and Communications*, vol. 117, p. 153133, 2020, doi: 10.1016/j.aeeu.2020.153133.
- [15] F. E. Mohmood and Y. E. M. Ali, "Study of the Impact of Antenna Selection Algorithms of Massive MIMO on Capacity and Energy Efficiency In 5G Communication Systems," *Al-Rafidain Engineering Journal (AREJ)*, vol. 26, no. 2, pp. 164-170, 2021, doi: 10.33899/rengj.2021.130499.1110.
- [16] M. A. Rahman, M. S. J. Singh, M. Samsuzzaman, and M. T. Islam, "A compact skull-shaped defected ground super wideband microstrip monopole antenna for short-distance wireless communication," *International Journal of Communication Systems*, vol. 33, no. 14, p. e4527, 2020, doi: 10.1002/dac.4527.
- [17] S. Shah *et al.*, "A compact dual-band semi-flexible antenna at 2.45 GHz and 5.8 GHz for wearable applications," *Bulletin of Electrical Engineering and Informatics*, vol. 10, no. 3, pp. 1739-1746, 2021, doi: 10.11591/eei.v10i3.2262.
- [18] T. T. Duong, S. Cao, and H. Duong, "An open double ring antenna with multiple reconfigurable feature for 5G/IoT below 6GHz applications," *Bulletin of Electrical Engineering and Informatics*, vol. 11, no. 1, 2022, doi: 10.11591/eei.v11i1.3337.
- [19] S. Santhanam and T. S. Palavesam, "Comparative characterization of microstrip patch antenna array with defected ground structure for biomedical application," *Bulletin of Electrical Engineering and Informatics*, vol. 11, no. 1, pp. 346-353, 2022, doi: 10.11591/eei.v11i1.3459.
- [20] M. Z. Rahman, K. C. D. Nath, and M. Mynuddin, "Performance Analysis of an Inset-Fed Circular Microstrip Patch Antenna Using Different Substrates by Varying Notch Width for Wireless Communications," *International Journal of Electromagnetics and Applications*, vol. 10, no. 1, pp. 19-29, 2020, doi: 10.5923/j.ijea.20201001.03.
- [21] M. Hussain *et al.*, "Simple wideband extended aperture antenna-inspired circular patch for V-band communication systems," *AEU-International Journal of Electronics and Communications*, vol. 144, p. 154061, 2022, doi: 10.1016/j.aeeu.2021.154061.
- [22] S. Kamal *et al.*, "Wheel-shaped miniature assembly of circularly polarized wideband microstrip antenna for 5G mmWave terminals," *Alexandria Engineering Journal*, vol. 60, no. 2, pp. 2457-2470, 2021, doi: 10.1016/j.aej.2020.12.054.
- [23] M. Y. Zeain *et al.*, "Design of a wideband strip helical antenna for 5G applications," *Bulletin of Electrical Engineering and Informatics*, vol. 9, no. 5, pp. 1958-1963, 2020, doi: 10.11591/eei.v9i5.2055.
- [24] M. J. Farhan and A. K. Jassim, "Design and analysis of microstrip antenna with zig-zag feeder for wireless communication applications," *Bulletin of Electrical Engineering and Informatics*, vol. 10, no. 3, pp. 1388-1394, 2021, doi: 10.11591/eei.v10i3.2122.
- [25] K.-L. Wong, "Compact and broadband microstrip antennas," *John Wiley & Sons*, 2004.





- [26] F. Mahbub, S. B. Akash, S. A. K. Al-Nahyun, R. Islam, R. R. Hasan and M. A. Rahman, "Microstrip Patch Antenna for the Applications of WLAN Systems using S-Band," *IEEE 11th Annual Computing and Communication Workshop and Conference (CCWC)*, 2021, pp. 1185-1189, doi: 10.1109/CCWC51732.2021.9376114.
- [27] R. H. Thaher, "Design and analysis microstrip antenna with reflector to enhancement gain for wireless communication," *Bulletin of Electrical Engineering and Informatics*, vol. 9, no. 2, pp. 652-660, 2020, doi: 10.11591/eei.v9i2.1696.
- [28] B. Sailaja and K. K. Naik, "CPW-fed elliptical shaped patch antenna with RF switches for wireless applications," *Microelectronics Journal*, vol. 111, p. 105019, 2021, doi: 10.1016/j.mejo.2021.105019.
- [29] C. Mukta, M. Rahman, and A. Z. M. T. Islam, "DESIGN OF A COMPACT CIRCULAR MICROSTRIP PATCH ANTENNA FOR WLAN APPLICATIONS," *International Journal on AdHoc Networking Systems (IJANS)*, vol. 11, no. 3, pp. 1-12, 2021. doi: 10.5121/ijans.2021.11301.
- [30] A. Atser, J. Môm, and L. Abiem, "Impact of Feed point location on the Bandwidth, Frequency and Return loss of Rectangular microstrip patch Antenna," *International Journal of Engineering Research and Technology*, vol. 2, pp. 1612-1616, 2013.
- [31] W. H. Weedon and S. K. Cheung, "Ku-band low-profile and wideband satellite communication antenna (LPWSA)," *IEEE International Symposium on Phased Array Systems and Technology (PAST)*, 2016, pp. 1-7, doi: 10.1109/ARRAY.2016.7832638.
- [32] T. Prabhu, E. Suganya, and S. C. Pandian, "Design and analysis of dual feed patch antenna at 3.5 GHz mid-band 5G technology," *International Journal of Intelligence and Sustainable Computing*, vol. 1, no. 3, pp. 267-279, 2021.
- [33] B. L. V. Kumar, C. B. Pramod, S. Nagendram, and S. Kalyan, "Design and Analysis of Circular Patch Antenna," *Journal of Physics: Conference Series*, 2021, vol. 1804, p. 012200, doi:10.1088/1742-6596/1804/1/012200.
- [34] N. Taher, A. Zakriti, N. Amar Touhami, and F. Rahmani, "Circular ring UWB antenna with reconfigurable notch band at WLAN/sub 6 GHz 5G mobile communication," *Microsystem Technologies*, pp. 1-8, 2022, doi: 10.1007/s00542-021-05246-9.
- [35] A. M. Taha and S. Shabunin, "Design Six Band patch Antenna for 5G and Radar Applications," *Ural Symposium on Biomedical Engineering, Radioelectronics and Information Technology (USBREIT)*, 2021, pp. 0185-0189, doi: 10.1109/USBREIT51232.2021.9455012.
- [36] M. V. Rao, B. Madhav, T. Anilkumar, and B. P. Nadh, "Metamaterial inspired quad band circularly polarized antenna for WLAN/ISM/Bluetooth/WiMAX and satellite communication applications," *AEU-International Journal of Electronics and Communications*, vol. 97, pp. 229-241, 2018, doi: 10.1016/j.aeue.2018.10.018.
- [37] D. M. Pozar, "Microstrip antennas," *Proceedings of the IEEE*, vol. 80, no. 1, pp. 79-91, 1992, doi: 10.1109/5.119568.
- [38] G. Ahmed, M. I. Babar, S. Ali, and F. Ali, "A wideband and efficient patch antenna with two different feeding mechanisms for Ku/K bands applications," *Mehran University Research Journal Of Engineering & Technology*, vol. 39, pp. 625-634, 2020, doi: 10.22581/muet1982.2002.17.
- [39] V. Saidulu, K. S. Rao, K. Kumarswamy, and P. S. Rao, "Dielectric SUPERSTRATE Thickness VARIATIONON the Characteristics of Circular Patch Antenna," *International Journal of Engineering Research & Technology*, vol. 2, no. 9, pp. 3003-3011, 2013.
- [40] S. Z. M. Hamzah, N. F. Abdul Malek, S. Y. Mohammad, F. N. Mohd Isa and M. R. Islam, "Design of circular patch antennas at mmWave," *8th International Conference on Computer and Communication Engineering*, 2021, pp. 144-149, doi: 10.1109/ICCCE50029.2021.9467213.
- [41] R. Sharma, N. S. Raghava and A. De, "Design of Compact Circular Microstrip Patch Antenna using Parasitic Patch," *6th International Conference for Convergence in Technology (I2CT)*, 2021, pp. 1-4, doi: 10.1109/I2CT51068.2021.9418104.
- [42] S. D. Sateaa, M. S. Hussein, Z. G. Faisal, and A. M. Abood, "Design and simulation of dual-band rectangular microstrip patch array antenna for millimeter-wave," *Bulletin of Electrical Engineering and Informatics*, vol. 11, no. 1, pp. 299-309, 2022, doi: 10.11591/eei.v11i1.3336.
- [43] S. Thakur and N. Singh, "Circular-slot THz antenna on PBG substrate for cancer detection," *Optik*, vol. 242, p. 167355, 2021, doi: 10.1016/j.matpr.2020.12.1014.
- [44] K. Jairath, N. Singh, V. Jagota, and M. Shabaz, "Compact ultrawide band metamaterial-inspired split ring resonator structure loaded band notched antenna," *Mathematical Problems in Engineering*, vol. 2021, no. 5174455, pp. 1-12, 2021, doi: 10.1155/2021/5174455.
- [45] K. Jairath and N. Singh, "A novel WLAN and X-band rejected elliptical slot loaded metamaterial inspired antenna," *Materials Today: Proceedings*, 2021, doi: 10.1016/j.matpr.2020.12.1014.

BIOGRAPHIES OF AUTHORS



Hiba A. Alsawaf     Mrs. Hiba has done her B.E in Electrical Engineering/Electronic and Communications Engineering from Mosul University. She received her master's degree in electronic and communication engineering from the same University and is currently pursuing her PhD in the field of Digital Communication Engineering. She has 11 years of teaching experience at Nineveh University/College of Electronics Engineering. She can be contacted at email: hiba.hmdoon@uoninevah.edu.iq.



Bushra Muhammed Ahmad     has done her B.E in Electrical Engineering/Electronic and Communications Engineering from Mosul University. She received her master's degree in 2012 in communication engineering from the same University. She has 11 years of teaching experience at Mosul University/College of Engineering. She can be contacted at email: Bushramuhammed@uomosul.edu.iq.